

# A Study on ZnO Nanoparticles Synthesized by Chemical Precipitation Method

Deepak Chaurasiya<sup>1\*</sup>, Dr. Satish Kumar<sup>2</sup>

<sup>1</sup> Research Scholar, Shri Krishna University, Chhatarpur M.P.

<sup>2</sup> Professor, Shri Krishna University, Chhatarpur M.P.

**Abstract** - Without the use of a capping agent, undoped ZnO and Ni- and Fe-doped ZnO nanoparticles were synthesised through chemical precipitation. To learn more about the structural, optical, vibrational, and electronic characteristics of the samples generated by the chemical precipitation approach, a wide range of characterisation techniques were applied to them. A model and mechanism for the remarkable structural alteration of Ni- and Fe-doped ZnO nanostructures were presented and discussed at length.

**Keywords** - Structural, Vibrational, Optical, Electronic Properties, ZnO Nanoparticles, Chemical Precipitation Method, etc.

-----X-----

## INTRODUCTION

For the average person, the term "Nanotechnology" needs no introduction, as it is advancing to new heights of grandeur at an alarming rate. The scientific community's desire to learn more about nanoscience and nanotechnology was sparked by the field's wide range of potential applications and the everyday need to reduce the size of gadgets. Since the field of nanoscience has evolved so much, it's difficult to pinpoint the exact year of its inception. There are numerous examples from ancient ayurvedic Indian literature, written between the 8th and 13th centuries AD, where the usage of nanomaterials, such as nanopowdered medications, was beneficial in the treatment of various diseases as "bhasmas." Many early examples of nanostructured materials were derived from the experimental perception and manipulation of materials by different smiths. Lycurgus Cup, (1) a Roman dichroic glass cage containing colloidal gold and silver nanoparticles, is an example from the fourth century. Another outstanding example of the employment of metallic nanoparticles is the use of sparkling and luminous ceramic pots. The employment of nanoparticles in stained glass windows in cathedrals as photocatalytic air purifiers is another example of nanomaterials usage in history. Carbon nanotubes and cementite nanowires were found to be responsible for the "Damascus" sabre blade's high tensile strength. Nanoscience and nanotechnology are being used in these situations without the practitioners being aware of the fact they are doing so. (2)

### The Effects at Nano-scale

A nanometer is the smallest unit of length in the world. Water molecules are around 0.3nm across, while red

blood cells are approximately 7000nm across. Since materials are expected to behave differently at a nanoscale, this is why people are interested in the subject matter. When compared to nanostructured materials, the characteristics of bulk materials frequently alter dramatically. Particles of ceramics or metals can be used to create composites that are far stronger than those predicted by present models. As an example, metals with grain sizes of 10nm or less are seven times more hard and tough than their typical counterparts with grain sizes in the hundreds of nanometers. The laws of quantum physics are responsible for a wide range of dramatic developments. A material's bulk properties are an average of all of its atoms' quantum physics, which affects its properties. We ultimately reach a point where the averaging no longer works as we shrink things farther and further. (3)

### Metal Oxides Nanomaterials

Researchers have been drawn to bulk metal-oxides and nanophase metal-oxide semiconductors for centuries. Its importance can be gauged by looking at the wide range of applications that stem from its key features. With its unique physical-chemical and transport properties that are distinct from those of larger, bulk materials, nanostructures are ideal for creating novel or superior optical, electrical or sensor devices. It has been more popular to synthesise inorganic metal-oxide nanostructures at low cost and with well-defined morphology because of their simplicity of manufacture and prospective uses. There is a lot of interest in adjusting the size and shape of nanomaterials in a variety of forms, such as nanowires, nano fibrils, rectangles, seeds, belts, and sheets. In the literature, a few examples

are given of alumina ( $\text{Al}_2\text{O}_3$ ), doped with metals, rare earths, garnets, borates, phosphates as bulk. (4)

## Introduction of Zinc Oxide

Group II-VI semiconductor nanostructures research continues at a steady pace. Wide band gap semiconductor nanomaterials' structure and morphology have long been a basic but tough goal because their properties are largely determined by their form, size, and distribution. Research into ZnO (semiconducting Zinc Oxide) has gained a lot of attention during the last few decades. Even in today's research, ZnO remains a significant wide band gap semiconductor (3.2 eV at 300K). When ZnO is reduced to nanoscale low-dimensional formations, it gains new and better technologically potent capabilities. (5) ZnO's large exciton binding energy (60meV) is one of the reasons for its significance in lasers based on excitonic recombination that operate above room temperature. The strong piezoelectric and pyroelectric capabilities of wurtzite structure, due to the lack of a centre of symmetry and substantial electromechanical coupling, lead to the usage of ZnO in mechanical actuators and piezoelectric sensors. ZnO shares some optical qualities with GaN, a wide band gap semiconductor that is frequently utilised in the manufacturing of ultraviolet, blue, green, and white light generating devices. Some interesting aspects of ZnO, such as a large exciton binding energy, greater radiation stability and the ability to obtain high quality ZnO bulk single crystals, make it an attractive alternative to GaN.

## Basic Properties of Zinc Oxide

### 1. Crystal Structure

wurtzite structure of ZnO belongs to  $P6_3mc$  space group symmetry. Cubic rocksalt, zinc blende, and wurtzite are the three ZnO formations that can be found. In the wurtzite phase, the thermodynamically stable structure is attained at ambient conditions. For wurtzite, zinc blende, and rock salt, total ground state energy was computed as a function of unit cell volume using a Hartee-Fock linear combination of atomic orbitals theory. (6)

### 2. Mechanical Properties

Hardness, stiffness, piezoelectric constants, Young's bulk modulus and yield strength are all aspects of mechanical qualities that can be studied. Hook's law was used to express stress components as a function of strain tensors. Linear combinations of elastic stiffness coefficients were used to better express this. An optical technique known as Brillouin zone scattering is employed to measure the elastic coefficients. By measuring the phase velocities in various directions, light scattering from Brillouin zones interacts with thermal excitations in materials, especially acoustic phonons in crystals. X-ray diffraction, energy dispersive X-ray diffraction, angular dispersive X-ray diffraction, and x-ray absorption spectroscopy are some of the

techniques used to estimate the pressure dependence of lattice parameters, as well. (7)

### 3. Thermal Properties

Thermal expansion coefficients for in-plane and out-of-plane instances are used to measure the lattice properties of semiconductors. Hexagonal ZnO lattice constants measured by thermal expansion coefficients at room temperature were found to be  $a/a=4.7510\text{-}6\text{K}^{-1}$  and  $a/c=2.910\text{-}6\text{K}^{-1}$  via capacitive techniques. Based on the synthesis methods, these properties are substantially dependent on thin films formed on substrates at varied pressure and growth temperatures. Due to the importance of substrate lattice characteristics and thermal expansion coefficients, metal oxides, in general, and ZnO in particular, may be critical in high temperature applications.

### 4. Electronic Band Structure

In order to construct ZnO-based LEDs and other optoelectronic devices, the band gap engineering of doped ZnO is crucial. Optical characteristics of bulk ZnO, due to its 3.2eV direct band gap and 2.45eV indirect band gap, have taken centre stage in recent years among researchers. In addition to higher breakdown voltages and the ability to withstand large electric fields, a wide band gap also provides advantages such as lower electronic noise, higher operating temperatures and powers, and more efficient photo-catalytic hybrid nanostructures for hydrogen generation. However, one drawback is the lack of p-type ZnO crystals, which are necessary for optoelectronic applications.

### 5. Defects Driven Properties

Impurities and flaws can drastically alter the characteristics of semiconductors, which are critical for electronic devices. A defect atom in a million host atoms is rarer than a defect atom needed to provide the desired attribute. Crystal structures contain a variety of defects, such as vacancies, interstitials, antisites, and so on. There are two types of common ZnO vacancies, depending on the synthesis settings, oxygen and zinc vacancies, respectively. As a result, under Zn-rich circumstances, oxygen vacancies ( $\text{V}_\text{O}$ ) are more prevalent due to their lower energy of creation compared to zinc interstitial ( $\text{Zn}_\text{i}$ ). Zinc vacancies ( $\text{V}_\text{Zn}$ ) dominate in oxygen-rich environments.

### 6. Optical Properties

Many faults in semiconductors may be traced back to changes in energy levels, therefore examining their optical properties is essential. Light Emitting Diodes (LEDs) and lasers based on GaN have transformed our daily lives in several ways. (8) Due to ZnO's significant advantages over GaN, such as its more efficient exciton emission in ZnO at ambient temperature and wide band gap, it has the potential

to replace GaN in semiconductor light emitting devices (3.32eV). As the size of the material shrinks to the nanoscale, it has an impact on its fluorescence qualities. At normal temperature, zinc oxide crystal's high exciton binding energy ensures efficient excitonic emission, resulting in UV illumination in disordered nanoparticles and thin films.

## 7. Vibrational Properties

It is impossible to rule out the potential of amorphous forms or very low amounts of crystalline phases in the sample material due to the detection limitations of X-ray diffraction (XRD). FTIR and Raman spectroscopy can be used to detect changes in the material. It is possible to detect a very little amount of a material in a sample using these methods. While FTIR spectroscopy has a sensitivity of 100 ppm, a very small cross section of material (i.e. 1 micrometre in diameter) can be analysed using Raman characterisation. FTIR and Raman data for bulk and nanosized ZnO may be found in a plethora of publications, some of which compare the results of different investigations. (9)

## Introduction of Copper Oxides

It is important to note that copper oxide has two distinct semiconductor phases: cupric oxide (CuO) and cuprous oxide (Cu<sub>2</sub>O). Due to the reduced surface potential barrier of copper (II) oxide (CuO), which has a monoclinic structure and an indirect band gap of between 1.4-1.85eV, it can dramatically impact field emission properties. Copper (I) oxide (Cu<sub>2</sub>O), a p-type semiconductor with a cubic crystal structure and a direct band gap of 2.2eV, is frequently used in solar cell fabrications and catalysis because of its excellent properties. CuO and monoclinic CuO unit cells can be used to better understand the crystal structure. (10)

## ZnO Nanoparticles

On the basis of literature survey, it is well established the overall properties of a larger system constituted of transition metal doped nanoparticles directly correlate with the magnetic and semiconducting capabilities of constituent nanoparticles. (11) This is critical to understanding many theoretical interpretations, such as spin correlation in DMS, as well as other phenomena. These findings allow for the experimental examination and creation of devices based on semiconductor magnetic nanostructures, as well. Research into transition metal-doped semiconductor nanostructures was spurred forward by the importance of such studies. It is possible to generate huge quantities of ZnO nanoparticles using a simple chemical precipitation process. These nanoparticles have already been tested for their properties in terms of structural, optical, and electrical properties. (12)

## OBJECTIVES OF THE STUDY

- The Investigation of structural, optical, vibrational, electronic properties of undoped

and TM doped (Ni, Fe) doped ZnO nanostructures synthesized by chemical precipitation

## RESEARCH METHODOLOGY

Different experimental techniques will be employed to synthesize and characterize the nanostructures. A chemical precipitation approach will be used to make undoped ZnO nanomaterials as well as Ni, Fe-doped ZnO nanomaterials. We will use a variety of characterization methods, including XRD, TEM, SEM, EDX, Micro-Raman spectroscopy (RS), UV-Visible spectroscopy, Photoluminescence (PL) spectroscopy, X-ray photoelectron spectroscopy (XPS), and Vibrating spectroscopy, to investigate the previously prepared nanomaterials, as well as the aforementioned prepared nanomaterials.

## Synthesis Methods

Pure ZnO and Ni, Fe doped ZnO nanostructures will be prepared by chemical precipitation route.

## Chemical Precipitation Method

When materials are obtained through chemical reactions in a solution and then precipitated, this is known as the chemical precipitation process. These characteristics make it the most useful and efficient method available. To make nanostructures, the chemical precipitation approach can be used. This is due to the high water solubility of the basic precursors, such as acetates, carbonates, and nitrates. The use of an ice bath and magnetic stirring allows for low temperature synthesis, which has an advantage over other methods.

## Characterization Techniques

Nonmaterials will be characterised using an array of microscopic and spectroscopic methods. Structure and composition of produced nanomaterials will be studied using X-ray diffractography (XRD), transmission electron microscopy (TEM), and scanning electron microscopy (SEM) equipped with Energy Dispersive X-ray Spectroscopy (EDS). In addition, UV-Visible (UV-Vis), Photoluminescence (PL), and X-ray Photoelectron Spectroscopy will be used to examine the nanomaterials' optical and electrical properties (XPS). When it came to studying vibrations, researchers used FTIR and micro-Raman Spectroscopy.

## 1. X-Ray Diffraction Technique

Compounds can be identified and quantified by using the non-destructive technique of XRD, which is a multi-purpose analytical technique that does not damage materials. The crystallite size and strain are shown in the XRD data acquired from the peak positions, the peak heights, the background bump and the amorphous content (peak widths). The

diffraction pattern acquired from an unknown material is compared to a recognized database containing reference patterns in order to make identification.

## 2. Electron Microscopy

The nanomaterials will be made of using electron microscopy. When it comes to resolution and magnification, electron microscopy has a unique advantage over optical microscopes. Morphological and elemental analyses will be performed using transmission and scanning electron microscopy, together with energy dispersive x-ray spectroscopy (EDS).

## 3. Micro-Raman Spectroscopy ( $\mu$ RS)

Molecules are influenced by photons, which change their energy states. The molecular system scatters a photon in Raman spectroscopy. It is known as Rayleigh scattering that most photons are elastically scattered. Photons in Rayleigh scattering have the same wavelength as those that are absorbed. Raman scattering occurs when molecules scatter light in an inelastic way. The Raman Effect is only a tiny fraction of the photons that are emitted.

## 4. Fourier Transform Infrared (FTIR) Spectroscopy

The presence or absence of specific functional groups linked to a molecule can be detected using Fourier transform infrared spectroscopy (FTIR). Wave numbers range from 4000 to 400  $\text{cm}^{-1}$  in the typical fingerprint region of the vibrational infrared spectrum. Most covalently bound molecules emit radiation with vibrational frequencies stretching and bending in this region. A change in dipole moment will only occur when IR radiation is absorbed at frequencies that match the IR energy of the molecules' natural vibrational frequencies. All frequencies are represented in a wave-like interferogram in FTIR. The Fourier transform is a mathematical procedure that separates the interferogram's individual absorption frequencies.

## 5. UV-Visible Spectroscopy

The absorption spectrum is the simplest and most straightforward approach for determining a semiconductor's band structure. In the absorption process, an electron is excited from lower to higher energy states by a photon of known energy. One can identify all potential electron transitions by examining the variations in transmitted or absorbed light.

## 6. Fluorescence Spectroscopy

Fluorescence spectroscopy will be used to test the produced nanomaterials for any additional optical transitions from electronic and vibrational states. Here, a specific wavelength (typically an excitation wavelength in the UV region with energy larger than or equal to the band gap) is used to excite nanomaterials from their ground state to a higher energy state.

Therefore, different energy of photons is emitted by nanomaterials as a result. To better understand how electronic and vibrational levels exist in nanomaterials, this emission spectra sheds light on the potential irradiations that may occur during relaxations.

## 7. X-Ray Photoelectron Spectroscopy (XPS)

X-ray for analyzing the chemical composition of solid surfaces, photoelectron spectroscopy (XPS), also known as electron spectroscopy of chemical analysis (ESCA), has received a lot of attention. In order to perform XPS surface analysis, a sample must be exposed to mono-energetic soft x-rays and the electrons generated by various processes must be detected.

## RESULTS

### Transmission Electron Microscopy (TEM) And Energy Dispersive X-Ray Spectroscopy (EDS) Analysis

In this transmission electron microscopy (TEM) picture of zinc oxide nanoparticles, their uneven shapes and average size of 30 nm are clearly visible. Figure 1's inset (a) demonstrates how aggregation of nanoparticles with a size of 30 nm is visible even in structures with a size of 100 nm or greater.

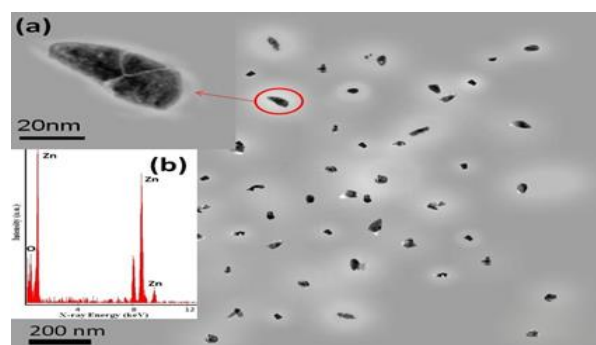


**Figure 1: ZnO nanoparticle transmission electron micrograph. Inset (a). Image that has been enlarged to show a 100 nm-wide aggregate of smaller ZnO nanoparticles (b) EDS spectrum of prepared nanoparticles**

These peaks correspond to emissions from the K-shell of oxygen (0.592 keV) and the L-shell of zinc (1.037 keV) in the X-ray spectrum. In reality, the L-shell emission recorded here at 1.037 keV may be interpreted as the superposition of the more often reported 1.021 keV and 1.044 keV photoelectron transitions in Zn 2p<sub>3/2</sub> and Zn 2p<sub>1/2</sub>. Zinc also emits X-rays with energies of 8.44 keV and 9.33 keV, respectively, from its K and K core shells.

**Table 1: Nanoparticle mass, atomic number and R % composition after preparation**

Elements	Wt%	At%	R-value (%)
O (K)	27.15	60.36	152.3
Zn (L)	72.85	39.64	

Our sample of produced ZnO nanoparticles has an R-value of 152.3%, with a Zn:O At% of 40:60. Zinc interstitials (Zni) and VO are the two most common types of defects in ZnO, which leads to the material being classified as an n-type semiconductor.

**Ray Diffraction (XRD) Analysis**

Figure 2 displays the X-ray diffraction pattern of produced ZnO nanoparticles in the range 20°-80°, recorded in the  $\theta$ -2 $\theta$  geometry.

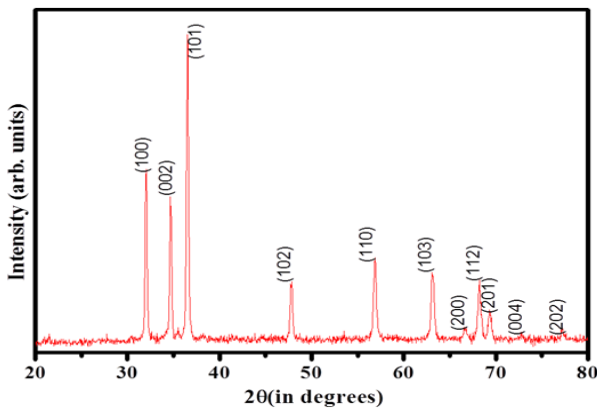


**Figure 2: The XRD  $\theta$ -2 $\theta$  scan of ZnO nanoparticles. ZnO hexagonal phase-corresponding Miller indices**

In Figure 2, a number of strong Bragg reflections are observed at 31.79°, 34.44°, 36.27°, 47.57°, 56.63°, 62.90°, 66.42°, 68.00°, 69.14°, 72.62° and 77.02° corresponding to (100), (002), (101), (102), (110), (103), (200), (112), (201), (004), (202), respectively. Here are presented peak positions that agree with those reported for the hexagonal wurtzite phase of ZnO, which has a space group of P63mc (JCPD 36-1451). The crystalline phase, lattice planes, and other features of the generated nanoparticles are determined using a comprehensive yet systematic XRD examination.

**Micro-Raman Spectroscopy ( $\mu$ RS) Analysis**

Crystalline and structural flaws in a material can be detected using Raman spectroscopy. Raman spectra are obtained in the range of 100-1200cm<sup>-1</sup> to ascertain the structural phase of produced nanoparticles and to investigate the presence of any flaws or contaminants inside the nanoparticles.

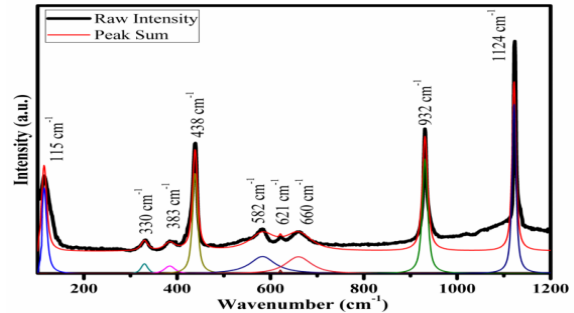


**Figure 3: Micro-Raman spectrum of deconvoluted ZnO nanoparticles with various peaks**

Figure 3 shows clearly discernible peaks at the frequencies of 115, 330, 383, 438, 582, 621, 660, 932, and 1124cm<sup>-1</sup>. The best fit to the Lorentzian-Gaussian (80%L, 20%G) functions under consideration was found by adjusting the FWHM and area of the nine peaks. Because of these tweaks, the total simulated peak profiles were the most accurate representation of the experimental data.

**Fourier Transforms Infrared (FTIR) Spectroscopy Analysis**

Nanoparticles have a larger surface area in relation to their volume. This ratio, known as the aspect ratio, is greater than that of bulk materials. Given that a nanoparticle's surface is where the majority of its molecules are located, studying its surface chemistry is crucial. We used FTIR spectroscopy to swiftly determine whether or not the various vibrational modes were present in the produced nanoparticles. ZnO nanoparticles' Fourier transforms infrared (4cm<sup>-1</sup>) spectra, measured in the frequency range of 370 to 7600 cm<sup>-1</sup>.

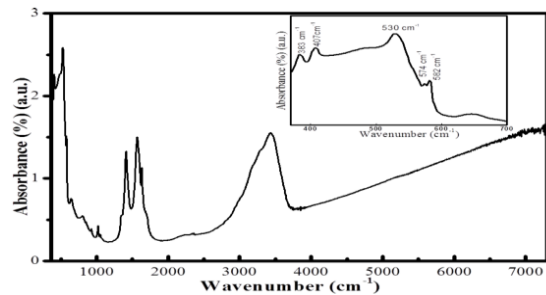


**Figure 4: ZnO nanoparticles' FTIR whole range spectrum, measured between 370 and 7600 cm<sup>-1</sup>**

**1. The expanded portion of the spectrum, shown in the inset, displays the Zn-O vibrational modes**

The hydroxyl (O-H) group of H<sub>2</sub>O stretches and bands at roughly 3400 and 1600 cm<sup>-1</sup>, respectively, as seen in Figure 4. This is because KBr pellets absorb moisture from the air during an FTIR experiment, causing these bands to emerge. We're particularly interested in the spectrums near infrared (NIR) region, where the vibrational modes of the metal-oxygen pair are hypothesised to be located. The FTIR spectra are examined between the wavelengths of 375 and 700cm<sup>-1</sup> to pinpoint the presence of such modes.

**X-Ray Photoelectron Spectroscopy (XPS) Analysis**

The complex electrical structure of solids may now be studied using two cutting-edge methods: X-ray photoemission and X-ray absorption spectroscopies. Because the procedure creates a positive hole, which then interacts with the freely moving conduction electrons, the resultant spectra do not accurately reflect the electronic states of the material.

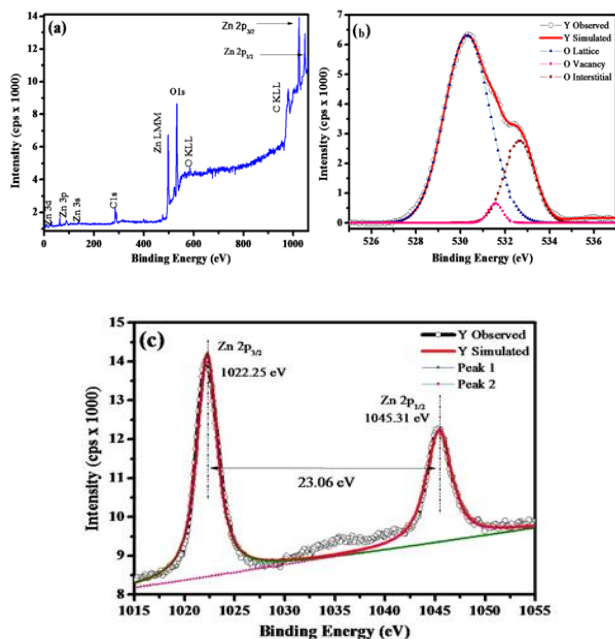


**Figure 5: (a) Spectrum of ZnO nanoparticles from an XPS scan. (b). XPS core level scan of O 1s. Deconvoluted profiles are used to demonstrate the existence of the OL, VO, and Oi states. (c) Zn 2p<sub>1/2</sub> and 2p<sub>3/2</sub> core level scans. Simulated profiles**

As can be seen in Figure 5, both zinc and oxygen release X-ray photoelectrons and Auger electrons in a number of distinct spectra (a). In this way, the XPS survey spectrum confirms that zinc and oxygen are the most prevalent elements and that the synthesised nanoparticles are completely free of any contaminants. Analyzing the core level XPS scan of O1 is crucial to understand more about the oxygen rich stoichiometry of the synthesised nanoparticles. By modelling the data at binding energies of 530.23 eV (blue solid triangular curve), 531.57 eV (pink solid squares curve), and

532.60 eV, we find that this peak profile may be deconvoluted into three separate Lorentzian-Gaussian (%80:20) profiles (brown solid circle curve). Three unique oxygen states are ascribed to locations in the crystal structure: the lattice site (OL) at 530.23 eV, the vacancy (VO) at 531.57 eV, and the interstitial (Oi) at 532.60 eV.

**UV-Visible Absorption Spectroscopy Analysis**

As structures are shrunk to the nanometer scale, the optical processes of absorption and emission in ZnO become more crucial. Radiative absorptions in ZnO nanoparticles were studied using UV-visible spectroscopy. ZnO nanoparticles' UV-visible absorption spectra in the scanning range of 300-450 nm is seen in Figure 6.

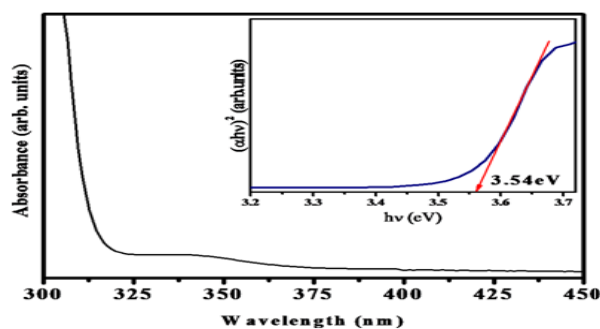


**Figure 6: Spectrum of UV-visible absorption in ZnO nanoparticles. Plot for (ahv)<sup>2</sup> vs. hv is also shown in the inset**

That maximal optical absorption occurs between 325 and 375 nm is shown. This indicates that size constraints have driven the absorption energy of ZnO nanoparticles towards the blue. Tauc's connection to the UV-visible absorption spectrum was used to generate a (hν)<sup>2</sup> vs. h plot, from which an estimate of the band edge absorption energy of the synthesised nanoparticles could be derived.

**Fluorescence (FL) Spectroscopy Analysis**

We employed fluorescence (FL) spectroscopy to investigate the size- and defect-state-related differences in the optical characteristics of produced ZnO nanoparticles, as well as to learn more about the band structure, component discrete states, and optical processes of excitation and emission. In order to get consistent excitation and emission slit widths of 2.5nm, we collected FL data across a wide range of wavelengths, from 285-700nm.

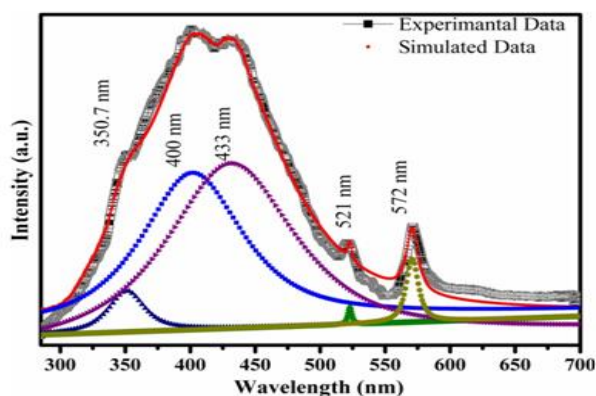


**Figure 7: ZnO nanoparticles' fluorescent emission spectrum shows strong agreement with calculated values**

To analyse and understand the diverse FL emissions of ZnO nanoparticles, it is helpful to de-convolute the experimental FL emission spectrum. Convolution of five separate emission spectra centred on 350.7nm, 400nm, 433nm, 521nm, and 572nm provides a good match to the experimentally observed FL emission spectrum of ZnO nanoparticles.

## CONCLUSION

The chemical precipitation approach will be used to synthesize and characterize structural, optical, vibrational, and electronic characteristics of ZnO nanostructures doped with transition metals (Ni, Fe). Chemical precipitation is used to create ZnO nanoparticles. There, the mechanism and process of ZnO nanoparticle generation will be clarified. The nanoparticles will be analyzed by TEM, EDS, XRD, Raman and FTIR, XPS, UV-visible and Fluorescence spectroscopy to determine their composition. The zinc and oxygen atoms in those 30nm nanoparticles will be discovered by TEM and EDS.

## REFERENCES

1. Mostoni, S, Pifferi, V, Falciola, L, Meroni, D, Pargoletti, E, Davoli, E & Cappelletti, G 2017, 'Tailored routes for home-made Bi-doped ZnO nanoparticles. Photocatalytic performances towards o-toluidine, a toxic water pollutant', *Journal of Photochemistry and Photobiology A: Chemistry*, vol. 332, pp. 534-545.
2. Kulkarni, SS, Sawarkar Mahavidyalaya, S & Shirsat, MD 2015, 'Optical and Structural Properties of Zinc Oxide Nanoparticles', *International Journal of Advanced Research in Physical Science*, vol. 2, no. 1, pp. 14- 18.
3. Rayerfrancis, A.; Bhargav, P.B.; Ahmed, N.; Chandra, B.; Dhara, S. *Physica B* 2015, 457, 96-102.
4. Shuxia Guo, Xingtang Zhang, Yabin Huang, Yuncai Li, Zuliang Du, *Chemical Physics Letters* 459 (2008) 82–84.

5. Lingling Zhang, Yulong Ding , Malcolm Povey , David York, *Progress in Natural Science* 18 (2008) 939–944
6. Li-Jian Bie, Xiao-Na Yan, Jing Yin, Yue-Qin Duan, Zhi-Hao Yuan, *Sensors and Actuators B* 126 (2007) 604-608.
7. T.S. Ko, S.Yang, H.C.Hsu, C.P.Chu, H.F.Lin, S.C.Liao, T.C.Lu, H.C Kuo, W.F.Hsieh , S.C.Wang, *Materials Science and Engineering*, B134 (2006) 54-58.
8. Hsiu-Fen Lin, Shin-Chieh Liao, Sung-Wei Hung, *Journal of Photochemistry and photobiology A; Chemistry* 174 (2005) 82-87.
9. Sarkar, D.; Tikku, S.; Thapar, V.; Srinivasa, R.S.; Khilar, K.C. *Colloid Surf., A* 2011, 381, 123-129.
10. K.C. Barick, Sarika Singh, M. Aslam, D. Bahadur, *Microporous and Mesoporous Materials* 134 (2010) 195–202.
11. Bai Shouli, Chen Liangyuan, Li Dianqing, Yang Wensheng, Yang Pengcheng, Liu Zhiyong, Chen Aifan, Chung Chiun Liu, *Sensors and Actuators B* 146 (2010) 129–137.
12. Yuan Zhang, Jiaqiang Xu, Qun Xiang, Hui Li, Qingyi Pan, and Pengcheng Xu, *J. Phys. Chem. C*, 113(2009)3430–3435.

---

## Corresponding Author

**Deepak Chaurasiya\***

Research Scholar, Shri Krishna University,  
Chhatrapur M.P.